JOURNAL OF MATERIALS SCIENCE 25 (1990) 1255–1260

Observations of an ordered Pd_7Eu phase in Pd–Eu alloys

K. TAKAO, K. L. ZHAO*, Y. SAKAMOTO
Department of Materials Science and Engineering, Nagasaki University, Nagasaki 852, Japan

The Pd–Eu alloys containing 6.1 to 14.3 at% Eu have been studied by metallographic examinations, X-ray diffraction, electron microscopic observations and electrical resistance measurements. The results for the annealed alloys indicate the presence of an ordered phase in the form of a Pd_7Eu superlattice, which is similar to the order found in Pd_7R (R = cerium, gadolinium, dysprosium, yttrium or samarium) previously. The order–disorder transition of the ordered Pd_7Eu phase in the alloys between Pd-10 and 16.6 (Pd_5Eu) at% europium alloys is accompanied with a peritectoid reaction: α-Pd + $Pd_5Eu \rightleftarrows Pd_7Eu$ at 850 ± 10 K. The ordering temperatures for Pd-6.1 and 7.5 at% Eu alloys are lower than the peritectoid reaction temperature, and they correspond to the solid solubility limit of europium in the α-Pd phase.

1. Introduction

The lattice parameters, magnetic susceptibilities and Mössbauer spectra of some Pd–Eu alloys have been examined by Harris and Longworth [1, 2]. In the Pd-rich alloys with less than 25 at% Eu, there is a linear variation of the room temperature lattice parameter with increasing europium content in the α-Pd solid solution alloys up to the solubility limit of about 10 at % Eu at about 873 K, in spite of the nominal size factor of europium with respect to palladium of 44%. The X-ray diffraction patterns of the alloys in the composition range 14 to 16 at% Eu indicate the presence of an intermediate phase corresponding to Pd_5Eu. The alloys at 18 and 20 at % Eu consist of a mixture of the Pd_5Eu and $L1_2$-type Pd_3Eu phases. Moreover, the lattice parameters, magnetic susceptibilities and Mössbauer isomer shifts indicated that the europium atoms are in the trivalent state in the solid solution alloys, the Pd_5Eu and in the Pd_3Eu phases.

Iandelli and Palenzona [3] have presented the binary Pd–Eu phase diagram determined by differential thermal analysis, X-ray diffraction, metallography and magnetic susceptibility measurements. On the Pd-rich side, there is the Pd_5Eu compound formed peritectically at 1378 K between the $L1_2$-type Pd_3Eu (m.p. = 1698 K) and liquid phases. A eutectic at about 12.5 at% Eu existing between the α-Pd and Pd_5Eu phases is observed at 1353 K.

Recent studies on a series of Pd-rich Pd-rare earth (R) alloys (R = cerium [4–6], yttrium [7, 8], gadolinium [9], dysprosium [8], samarium [10], holmium [11] and erbium [11]) have shown that the presence of an ordered Pd_7R phase which is isomorphous with a Pt_7Cu [12] is observed both from electron diffraction and electrical resistance measurements. However in the phase diagram of Pd–Eu alloy [3], no evidence was presented for the ordered Pd_7Eu phase. The ordered structure is a derivative of the $L1_2$-type Pd_3R phase [4–9] and/or of Pd_5R (R = samarium) [10], and formation of the Pd_7R phase has been found to be accompanied by a peritectoid reaction [8–10]:

$$\alpha\text{-Pd} + L1_2\text{-type } Pd_3R$$
$$(\text{or } Pd_5R \text{ (R = samarium)}) \rightleftarrows Pd_7R$$

The present work represents a continuation of studies on the ordered Pd_7R phase and on the associated order–disorder transition in a series of palladium-based alloys containing a substitutional rare-earth metal. In the present work the solute element is europium. As previous studies [1–3] of the Pd–Eu alloys indicate, as far as the $L1_2$-type Pd_3Eu and Pd_5Eu phases are concerned in the phase diagram, which is similar to that of Pd–Sm alloys determined previously [10, 13, 14], the existence of the ordered Pd_7Eu phase would also be expected.

2. Experimental procedures

Palladium-rich Pd–Eu alloys were studied by metallographic examination, X-ray diffraction, electron microscopic observation and electrical resistance measurement.

The palladium used was obtained from Tanaka Matthey K.K., with a purity of 99.95 wt %, and the europium was obtained from Rare Earth Products Ltd, of grade 99.9 wt %. The Pd–Eu alloys were prepared by argon arc-melting the appropriate weights of the constituent metals in a non-consumable electrode furnace. The alloy compositions used in this study were Pd-6.1, 7.5, 10.0, 11.2, 12.2, 13.3 and 14.3 at % Eu. After homogenization of the arc-melted alloy buttons, they were rolled to a thickness of about 100 to 200 μm except for the higher-europium-content

*On leave from Shandong Institute of New Materials, Jinan, People's Republic of China.

0022–2461/90 $03.00 + .12

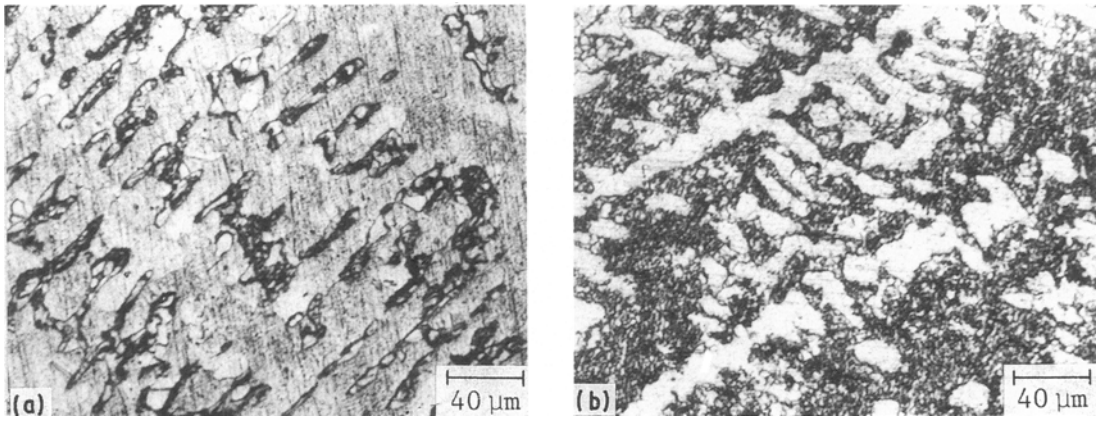

Figure 1 Micrographs of annealed Pd-12.2 at % Eu (a) and Pd-13.3 at % Eu (b) alloys.

alloys. The latter being brittle were cut with a microcutter into samples which were used in X-ray diffraction, electron microscopic observation and electrical resistance measurement [7–10].

Prior to measurement of the physical properties, the following heat treatments were performed:

1. The alloy samples were quenched into ice-water from about 1193 K for 10 min, simultaneously breaking the pre-evacuated and sealed-off silica tubes containing the samples with zirconium foils at room temperature. Before using these samples for measurements of X-ray lattice parameters and electrical resistance, the surfaces were abraded with fine emery paper in order to remove the oxide formed during quenching. These samples will be referred to as 'quenched'.

2. Some of the quenched samples were re-heated to about 1100 K *in vacuo* and then cooled to room temperature at a rate of 50 K h^{-1}. These samples will be referred to as 'annealed'.

The metallographic examination was carried out, after polishing, by etching in a mixture of H_2SO_4: HNO_3: H_2O = 2:2:1 by volume. The X-ray measurements were carried out at 298 ± 1 K using Cu$K\alpha$ radiation with a nickel filter. The lattice parameters were refined using a Nelson–Riley extrapolation function [15]. Electron diffraction patterns and electron micrographs were taken with a Hitachi H-800 electron microscope, after jet-electropolishing the disc samples in a solution of 1 vol perchloric acid and 4 vols acetic acid. The electrical resistance measurements were carried out *in vacuo* by heating and subsequently cooling the samples in the temperature range from 300 to 1100 K. A conventional four-point technique was employed, the current used was 100 mA, and the heating and cooling rates were 50 K h^{-1}.

3. Results and discussion

3.1. Metallographic examination and X-ray diffraction study

The metallographic examinations and X-ray diffractions indicated that both quenched and annealed alloys containing up to 10.0 at % Eu have only fcc α-Pd single phase, whereas for both quenched and annealed samples of Pd-11.2 and 12.2 at % Eu alloys, there was a eutectic structure consisting of α-Pd and Pd_5Eu phases, in addition to the primary dendritic α-Pd phase. Moreover, for both heat-treated samples of Pd-13.3 and 14.3 at % Eu alloys, the eutectic structure was also observed together with a dendritic structure of Pd_5Eu which was peritectically formed. These observations are in agreement with the phase diagram of Pd–Eu alloy studied by Iandelli and Palenzona [3]. Figures 1a and b show the micrographs of the annealed Pd-12.2 and 13.3 at % Eu alloys, respectively.

The lattice parameters of the α-Pd phase determined for both quenched and annealed Pd–Eu alloys are summarized in Table I. By comparison with previous results [1, 16] for low-europium-content alloys, there is an almost linear increase in the lattice parameters with increasing europium content up to about 10.0 to 11.2 at % Eu, and the lattice parameter values of the annealed alloys are slightly smaller than those of the quenched alloys.

Even if these alloys were to have an ordered Pd_7Eu phase, which is expected within the phases, it would be impossible to detect the superlattice reflections by X-rays because they are quite weak due to the small difference in the atomic scattering factors of the component atoms and because of the large absorption coefficient.

Figure 2 shows X-ray diffraction patterns of both

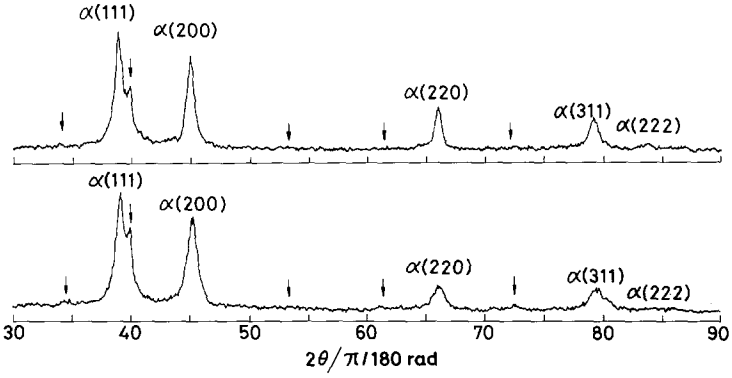

Figure 2 X-ray diffraction line profiles for both quenched (upper) and annealed (lower) Pd-14.3 at % Eu alloys at room temperature. Arrows indicate diffraction lines of Pd_5Eu phase. A Cu$K\alpha$ radiation with a nickel filter was used.

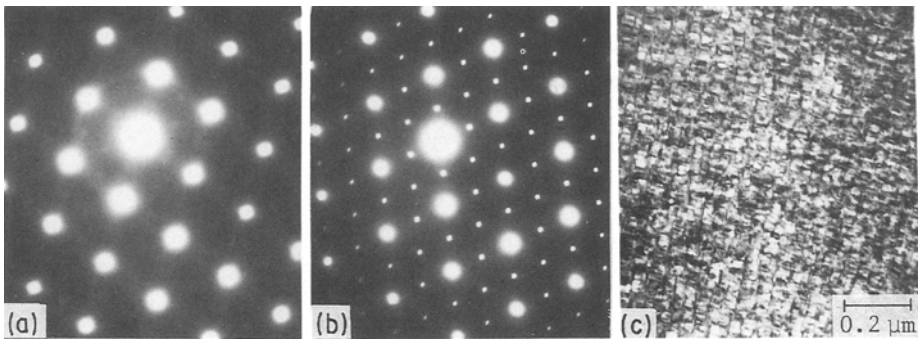

Figure 3 The [1 0 1] electron-diffraction patterns of quenched and annealed Pd-10.0 at % Eu alloys, and the dark-field image of the Pd_7Eu in the annealed alloy. (a) Quenched; (b) annealed; (c) taken with reflection around $(\frac{1}{2}\frac{1}{2}\frac{1}{2})$.

quenched (upper) and annealed (lower) Pd-14.3 at % Eu alloys. There are several reflections (↓) due to the Pd_5Eu phase, together with those of the α-Pd phase, and especially the reflection of Pd_5Eu around 2θ = 39.5 to 40° is strong. As found previously for Pd_5Sm [10] and Pd_5Ce [17, 18] phases, it can be seen that the Pd_5Eu phase also does not have a simple crystal structure of hexagonal $CaCu_5$-type unit cell [19, 20], as there are some discrepancies in the X-ray diffraction peak positions which were simulated by assuming the same crystal structure of a hexagonal $CaCu_5$ [19, 20]. The crystal structure of Pd_5Eu is considered to have similarly a two- or three-block structure as well as the Pd_5Sm [10] and H-Pd_5Ce [17, 18] phases, in which each block is made of two $CaCu_5$-type layers of a hexagonal symmetry [21, 22].

3.2. Electron microscopic observations

Electron diffraction patterns of quenched alloys in the composition range between 6.1 and 10.0 at % Eu exhibited mainly the fundamental reflections from the α-Pd solid solution, although at some points of the Pd-10.0 at % Eu alloy sample, faint superlattice reflections due to the Pd_7Eu phase were observed. Whereas for annealed alloys of the same compositions, the diffraction patterns exhibited superlattice reflections due to the expected Pd_7Eu phase, in addition to the fundamental reflections from the α-Pd phase, although the superlattice reflections for the low europium content alloys were quite faint.

Figures 3a and b show the [1 0 1] diffraction patterns for the quenched and annealed Pd-10.0 at % Eu alloys, respectively. It can be clearly seen from Fig. 3b that there are superlattice reflections at $(\frac{1}{2}\frac{1}{2}\frac{1}{2})$ and (1 0 0) positions and their equivalent, in addition to the fundamental reflections at the (1 1 1) and (2 0 0) positions in the f c c reciprocal lattice space. Thus, the form of the superlattice is found to be isomorphous with the previously determined Pd_7R (R = cerium, yttrium, gadolinium, dysprosium, samarium) [4–10]. Figure 3c shows a dark-field image taken with reflection from the mainly $(\frac{1}{2}\frac{1}{2}\frac{1}{2})$ plane in Fig 3b. The ordered domains are blocked and relatively small.

For quenched alloys in the composition range Pd-11.2 to 14.3 at % Eu, some places exhibited mainly fundamental reflections due to the α-Pd phase, in part by accompanying with the faint superlattice reflections of Pd_7Eu structure, but in other places showed the diffraction patterns with a hexagonal symmetry due to the Pd_5Eu phase. However, for annealed alloys the existence of the Pd_7Eu phase at some points was clearly observed, and at other points the reflections due to Pd_5Eu phase were also observed.

Figure 4a shows a typical example of a diffraction pattern taken with an incident beam parallel to the [0 0 1] direction for the Pd_5Eu phase in quenched Pd-11.2 at % alloy, and Fig. 4b shows the bright-field image. The diffraction pattern consists of the normal h c p reflections and the superlattice reflections at the positions of one-third or two third of the distance from the origin to $(1\bar{2}0)$ spots. The satellite spots around the strong main spots (1 0 0), $(1\bar{1}0)$ and $(1\bar{2}0)$ are considered to be due to overlapping of the two crystals with slightly different lattice constants, that is, due to some modifications of the crystal structure. The form of the superlattice is identified to be similar to the previously reported Pd_5Sm [10] and Hi-Pd_5Ce [17, 18] phases. As can be seen from Fig. 4b, there is some

TABLE I Lattice parameters of the α-Pd phase in several Pd–Eu alloys at 298 K

Alloys	Quenched† (±0.0002 nm)	Annealed‡ (±0.0001 nm)
6.1 at % Eu	0.3946	0.3939
7.5 at % Eu	0.3955	0.3951
10.0 at % Eu	0.3982	0.3978
11.2 at % Eu*	0.3990	0.3988
12.2 at % Eu*	0.3991	0.3993
13.3 at % Eu*	0.3996	0.3993
14.3 at % Eu*	0.3994	0.3997

*The α-Pd phase is co-existent with the Pd_5Eu phase.
†All alloy samples were rapidly quenched into ice-water from 1193 K.
‡The above quenched samples were re-heated to about 1100 K *in vacuo* at a heating rate of 50 K h^{-1}, then cooled to room temperature at the same rate.

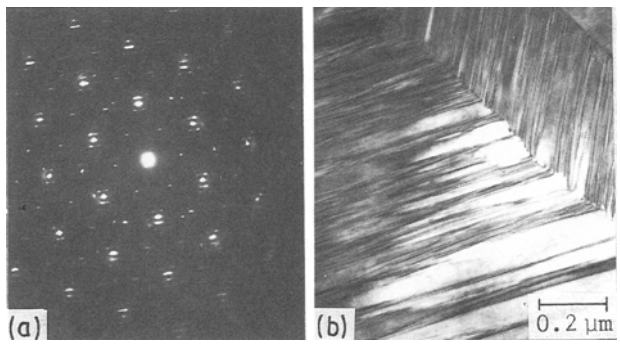

Figure 4 Electron diffraction pattern (a) for Pd_5Eu phase in quenched Pd-11.2 at % Eu alloy, and (b) the bright field image. Beam along [0 0 1].

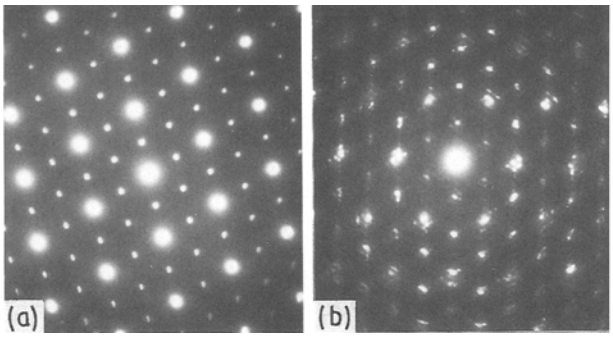

Figure 5 Electron diffraction patterns for (a) Pd_7Eu phase and (b) Pd_5Eu phase in annealed Pd-12.2 at % Eu alloy. Beams along (a), [1 0 1]; (b), [0 0 1].

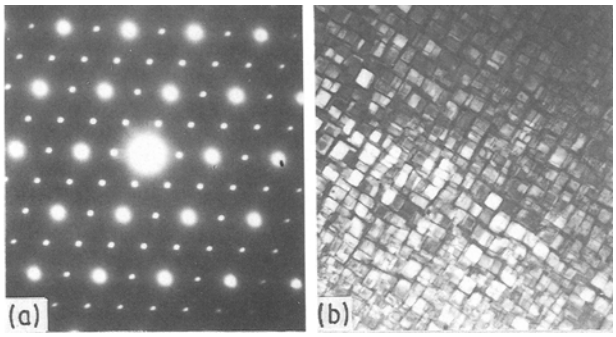

Figure 7 The [1 0 1] electron diffraction pattern (a) for Pd_7Eu phase in annealed Pd-14.3 at % Eu alloy, and (b) the dark field image taken with reflection around $(\frac{1}{2}\,\frac{1}{2}\,\frac{1}{2})$.

systematic introduction of crystallographic shear planes, which are due to the existence of stacking faults of the blocks [21, 22].

Figures 5a and b show the diffraction patterns of the Pd_7Eu and Pd_5Eu phases which co-existed in the annealed Pd-12.2 at % Eu alloys, respectively. As previously proposed for the formation of ordered Pd_7Sm phase [10], if the ordered Pd_7Eu phase is also formed by the peritectoid reaction at a certain temperature (α-Pd + $Pd_5Eu \rightleftarrows Pd_7Eu$), the Pd_5Eu phase should not exist in the annealed alloys containing 11.2 and 12.2 at % Eu, which are hypoperitectoid composition. However, the existence of Pd_5Eu phase in the annealed alloys is clear, which implies that the peritectoid reaction takes a long time to achieve complete equilibrium in the alloys.

Figures 6a and b show the diffraction patterns at different points of quenched Pd-14.3 at % Eu alloys. In addition to the Pd_5Eu phase (Fig. 6b), there is a co-existence of the ordered Pd_7Eu phase with the $L1_2$-type Pd_3Eu phase, because as seen from Fig. 6a, the (1 0 0), (1 1 0) and equivalent superlattice reflections of the ordered Pd_7Eu phase seem to overlap with those of the $L1_2$-type Pd_3Eu phase. Similar diffraction patterns have also been observed for quenched Pd-13.3 at % Eu alloy. This implies that the peritectic reaction [3] between the $L1_2$-type Pd_3Eu and liquid phases was not completely achieved, despite a hypoperitectic composition and relatively high temperature, and that the formation of the ordered Pd_7Eu phase occurs in part during quenching. As mentioned above, this suggests that although the initiation of ordering to the Pd_7Eu phase by accompanying with the peritectoid reaction is relatively fast, it takes a long time to achieve complete equilibrium.

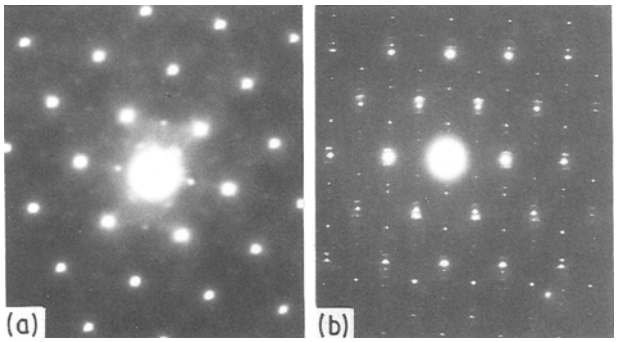

Figure 6 Electron diffraction patterns of quenched Pd-14.3 at % Eu alloy. Beams along (a), [1 0 1]; (b), [0 0 1].

Figure 7 shows the [1 0 1] diffraction pattern and the dark-field image taken around the $(\frac{1}{2}\,\frac{1}{2}\,\frac{1}{2})$ plane of the annealed Pd-14.3 at % Eu alloy. In spite of relatively high europium content, the formation of the ordered Pd_7Eu phase is clear, and the annealed alloy is certainly in a two-phase co-existence of the Pd_7Eu and Pd_5Eu phases. The ordered domains are large compared to those in the Pd-10.0 at % Eu alloy.

3.3. Electrical resistance measurement

The order–disorder transition for the Pd_7Eu phase was followed by measuring the resistance changes with temperature. The results for both initially quenched (a) and annealed (b) samples of the Pd–Eu alloys are shown in Fig. 8, as a resistance ratio, R_t/R_0, against temperature, where R_0 is the initial resistance at the starting temperature.

Showing a typical resistance ratio against temperature relationship, the quenched Pd-12.2 at % Eu alloy (in which the α-Pd phase co-existed initially with the Pd_5Eu phase at room temperature) commences to order into the Pd_7Eu at about 600 K. The ordered Pd_7Eu phase starts to re-disorder at about 750 K, leading to a disordered state at about 850 K, that is, the co-existence of α-Pd and Pd_5Eu phases. It can be seen from R_t/R_0 data of subsequent cooling process that the re-ordering starts at about 850 $\pm$ 10 K, which corresponds to the order–disorder transition temperature, T_c, for the α-Pd + $Pd_5Eu \rightleftarrows Pd_7Eu$.

In the heating and subsequent cooling relationship for the annealed sample which initially consisted of the ordered Pd_7Eu, α-Pd and, in part, the Pd_5Eu phase at room temperature, there is also a clear increase in the resistance at about 750 K, and the disordering to the α-Pd and Pd_5Eu phases is complete by T_c = 8500 K. On cooling, the re-ordering to the Pd_7Eu phase can also be seen with relatively small hysteresis. The T_c value is almost the same as those of the alloy compositions between Pd-10.0 and 14.3 at % Eu. The extrapolated resistance of the quenched alloys (disordered) to room temperature gives $R_{disorder}/R_{order}$ = 1.3 to 1.5.

On the other hand, the change in resistance due to the order–disorder transition for the Pd-6.1 and 7.5 at % Eu alloys is much smaller than that for the

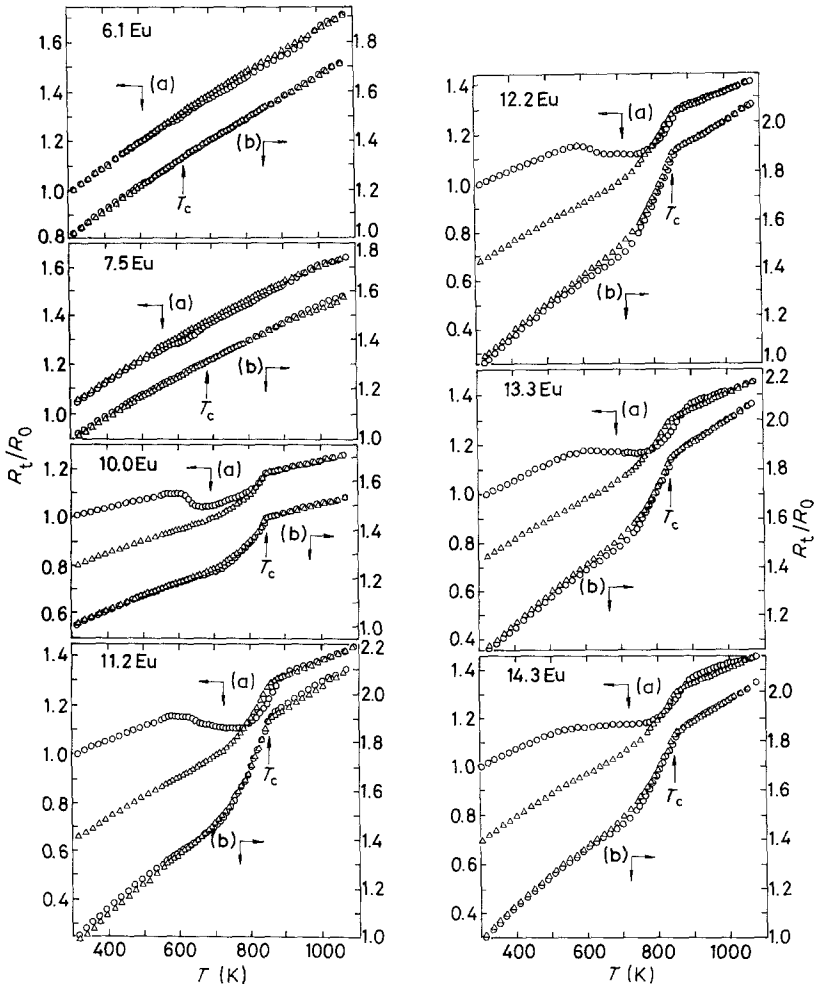

Figure 8 Electrical resistance ratio, R_t/R_0, against temperature for both initially quenched and annealed Pd–Eu alloys on heating and subsequently cooling. (a) Quenched; (b) annealed; ○, heating; △, cooling.

higher-europium-content alloys. The order–disorder transition temperatures were $T_c = 620 \pm 10$ K for Pd-6.1 at % Eu alloy; and $T_c = 680 \pm 10$ K for Pd-7.5 at % Eu alloy.

It is evident from the results of the metallographic examinations, the X-ray and electron microscopic observations and the resistometry that the formation of the ordered Pd_7Eu phase is accompanied by a peritectoid reaction: α-Pd + $Pd_5Eu \rightleftarrows Pd_7Eu$ at 850 ± 10 K for the alloy compositions of 10 to 16.6 at % Eu (Pd_5Eu); and for the alloys with less than about 10 at % Eu, the phase transition of α-Pd $\rightleftarrows$ α-Pd + Pd_7Eu takes place. The transition temperatures correspond to those of the solid solubility limit of europium in the α-Pd solid solution below the peritectoid reaction temperature. The results are quite similar to those for the previously reported Pd–Sm alloys [10].

The order–disorder transition temperatures of the Pd_7Eu phase and the solid solubility limit of europium in the α-Pd phase, determined from the resistance measurements, are shown with open circle symbols and dashed lines in Fig. 9. The full lines are based on the palladium-rich side of the phase diagram of the Pd–Eu alloy studied by Iandelli and Palenzona [3]. The peritectoid reaction temperature for the formation of the Pd_7Eu phase is higher than that of Pd_7Sm ($T_c = 820 \pm 10$ K [10]), but is lower than that of Pd_7Ce ($T_c = 960 \pm 5$ K [6]) determined from a similar cooling process of resistometry. The difference in the T_c value may be caused by the magnitude of atomic sizes and/or electronegativities of the atomic species. Detailed examinations are presently in progress.

4. Conclusions

The presence of an ordered phase having a Pd_7Eu superlattice structure for annealed Pd–Eu alloys in the composition range Pd-6.1 and 14.3 at % Eu was observed. The superlattice is isomorphous with that of

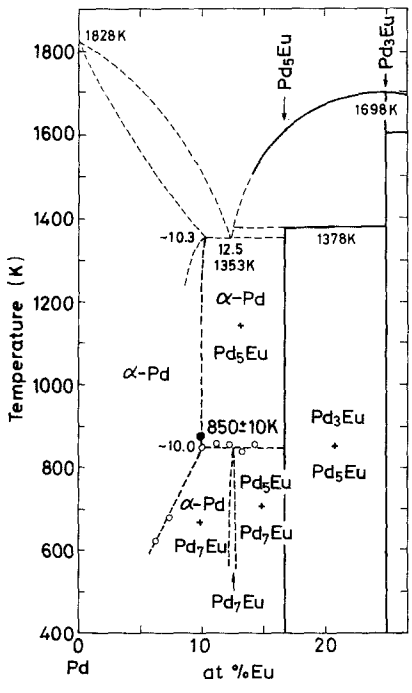

Figure 9 Phase diagram of the Pd-rich side of the Pd–Eu system. Solid lines and fine dashed lines from Iandelli and Palenzona [3], solid circle (873 K at 10 at % Eu), reported solubility of europium in palladium [1], open circles and heavy dashed lines represent data from the present study.

the previously reported Pd_7R (R = cerium, gadolinium, dysprosium, yttrium, samarium) [4–10].

The order–disorder transition of the Pd_7Eu phase in Pd-10 to 16.6 at % Eu (Pd_5Eu) is accompanied with a peritectoid reaction: α-Pd + $Pd_5Eu \rightleftarrows Pd_7Eu$ at $T_c = 850 \pm 10$ K.

The transition temperature for lower-europium-content alloys, Pd-6.1 and 7.5 at % Eu, decreases with decreasing europium content, which corresponds to the solid solubility limit of europium in the α-Pd phase.

References

1. I. R. HARRIS and G. LONGWORTH, *J. Less-Common Metals* **23** (1971) 281.
2. G. LONGWORTH and I. R. HARRIS, *ibid.* **33** (1973) 83.
3. A. IANDELLI and A. PALENZONA, *ibid.* **38** (1974) 1.
4. N. KUWANO, T. SHIWAKU, Y. TOMOKIYO and T. EGUCHI, *Jpn. J. Appl. Phys.* **20** (1981) 1603.
5. D. A. SMITH, I. P. JONES and I. R. HARRIS, *J. Mater. Sci. Lett.* **1** (1982) 463.
6. Y. SAKAMOTO, T. B. FLANAGAN and T. KUJI, *Z. Phys. Chem. N.F.* **143** (1985) 61.
7. Y. SAKAMOTO, M. YOSHIDA and T. B. FLANAGAN, *J. Mater. Res.* **1** (1986) 781.
8. K. TAKAO, Y. SAKAMOTO, M. YOSHIDA and T. B. FLANAGAN, *J. Less-Common Metals* **152** (1989) 115.
9. Y. SAKAMOTO, K. TAKAO, M. YOSHIDA and T. B. FLANAGAN, *ibid.* **143** (1988) 207.
10. Y. SAKAMOTO, K. TAKAO, S. TAKEDA and T. TAKEDA, *ibid.* **152** (1989) 127.
11. Y. SAKAMOTO, K. TAKAO and Y. NAGAOKA, (unpublished data).
12. A. SCHNEIDER and U. ESCH, *Z. Elektrochem.* **50** (1944) 290.
13. O. LOEBICH Jr and E. RAUB, *J. Less-Common Metals* **30** (1973) 47.
14. R. G. JORDAN and O. LOEBICH Jr, *ibid.* **39** (1975) 55.
15. J. P. NELSON and D. P. RILEY, *Proc. Phys. Soc. Lond.* **57** (1945) 160.
16. F. L. CHEN, M. FURUKAWA and Y. SAKAMOTO, *J. Less Common Metals* in press.
17. N. KUWANO, I. HIROSHIGE, Y. TOMOKIYO and T. EGUCHI, in Proceedings of the 7th International Conference on HVEM, Berkeley (1983) p. 291.
18. M. ITAKURA, Y. HISATSUNE, H. SATO, N. KUWANO and V. K. OKI, *Jpn. J. Appl. Phys.* **27** (1988) 684.
19. W. HAUCKE, *Z. Anorg. all. Chem.* **244** (1940) 17.
20. Th. HEUMANN and M. KNIEPMEYER, *ibid.* **290** (1950) 191.
21. P. RAO and R. P. GOEHNER, *J. Appl. Cryst.* **7** (1974) 482.
22. S. TAKEDA, H. HORIKOSHI and Y. KOMURA, *J. Microsc.* **129** (1983) 347.

Received 22 March
and accepted 20 June 1989